

# M<sup>3</sup>-20M: A Large-Scale Multi-Modal Molecule Dataset for AI-driven Drug Design and Discovery

Siyuan Guo,<sup>†</sup> Lexuan Wang,<sup>†</sup> Chang Jin,<sup>†</sup> Jinxian Wang,<sup>‡</sup> Han Peng,<sup>†</sup> Huayang Shi,<sup>†</sup> Wengen Li,<sup>†</sup> Jihong Guan,<sup>\*,†</sup> and Shuigeng Zhou<sup>\*,‡</sup>

<sup>†</sup>*Department of Computer Science and Technology, Tongji University, Shanghai, China*

<sup>‡</sup>*Shanghai Key Lab of Intelligent Information Processing, and School of Computer Science, Fudan University, Shanghai, China*

E-mail: [jhguan@tongji.edu.cn](mailto:jhguan@tongji.edu.cn); [sgzhou@fudan.edu.cn](mailto:sgzhou@fudan.edu.cn)

## Abstract

This paper introduces M<sup>3</sup>-20M, a large-scale Multi-Modal Molecular dataset that contains over 20 million molecules. Designed to support AI-driven drug design and discovery, M<sup>3</sup>-20M is 71 times more in the number of molecules than the largest existing dataset, providing an unprecedented scale that can highly benefit training or fine-tuning large (language) models with superior performance for drug design and discovery. This dataset integrates one-dimensional SMILES, two-dimensional molecular graphs, three-dimensional molecular structures, physicochemical properties, and textual descriptions collected through web crawling and generated by using GPT-3.5, offering a comprehensive view of each molecule. To demonstrate the power of M<sup>3</sup>-20M in drug design and discovery, we conduct extensive experiments on two key tasks: molecule generation and molecular property prediction, using large language models including GLM4, GPT-3.5, and GPT-4. Our experimental results show that M<sup>3</sup>-20M can significantly boost model performance in both tasks. Specifically, it enables

the models to generate more diverse and valid molecular structures and achieve higher property prediction accuracy than the existing single-modal datasets, which validates the value and potential of M<sup>3</sup>-20M in supporting AI-driven drug design and discovery.

The dataset is available at <https://github.com/bz99bz/M-3>.

## Introduction

Drug design and discovery is an important field in pharmacy, which aims to identify new therapeutic compounds and optimize their properties for clinical use.<sup>1-5</sup> This process involves the prediction of molecule-target interactions<sup>6-9</sup> and molecular properties,<sup>10-13</sup> and the design or generation of targeted molecules,<sup>14-18</sup> which are fundamental for developing effective and safe drugs. In recent years, various models trained or pre-trained and fine-tuned using massive data, such as,<sup>19-27</sup> have emerged as powerful tools in this domain. These models leverage large datasets and sophisticated algorithms to generate new compounds, predict molecular structures, and analyze their biochemical properties, significantly advancing the process of drug design and discovery. However, most existing molecular datasets for model training are limited to single-modality, failing to capture the characteristics of molecules completely, thus hampering the building of powerful models for drug design and discovery.

Recent works<sup>23,28,29</sup> have been paying increasing attention to multi-modal molecule datasets. Zeng<sup>29</sup> introduced a deep-learning system that bridges molecular structures and biomedical texts, achieving comprehension comparable to human professionals. Liu et al.<sup>28</sup> developed a multi-modal model for text-based retrieval and editing of molecular structures, facilitating advanced molecular text analysis. Liu et al.<sup>23</sup> presented a multi-modal large language model for molecular science that integrates graphs, images, and texts to support various downstream tasks. However, datasets used in these works still suffer from significant limitations. On the one hand, these datasets are typically small in size, encompassing a limited chemical space that restricts the generalization power of the trained or tuned models. On the other hand, the absence of complete modalities of molecular data undermines the

performance of computational models.

To address these limitations, this paper presents a new and large-scale multi-modal integrated molecule dataset called M<sup>3</sup>-20M for AI-driven drug design and discovery. M<sup>3</sup>-20M contains more than 20 million molecules with their SMILES strings, 2D graphs, 3D structures, physicochemical properties, and textual descriptions, providing unprecedented data scale, diversity, and comprehensiveness for training models of superior performance for various drug design and discovery downstream tasks. Concretely, M<sup>3</sup>-20M is 71 times more in the number of molecules than the largest existing dataset.<sup>28</sup> It collects physicochemical properties from the PubChem database<sup>30</sup> and enriches the description texts of molecules by both web crawling and GPT-3.5 generation. Therefore, each molecule’s SMILES corresponds to its 2D graph and 3D structure, physicochemical properties, and description texts. Figure 1 shows some examples from our M<sup>3</sup>-20M dataset.

In summary, M<sup>3</sup>-20M stands out of the existing datasets in at least the following three aspects: 1) **Large scale**: it contains over 20 million molecules, which is the largest open-access multi-modal molecule dataset for AI-driven drug design and discovery, to the best of our knowledge. 2) **Comprehensive modalities**: M<sup>3</sup>-20M boasts a more complete range of modalities, including one-dimensional molecular SMILES strings, two-dimensional molecular graphs, three-dimensional molecular structures, physicochemical properties, and textual descriptions. Such multi-modal data offers a holistic perspective of each molecule, benefiting model training and tuning for drug design and discovery. Additionally, we offer tools to generate 2D molecular graph images that facilitate compound patent retrieval, and to crawl PubMed for research articles related to specific molecules, thereby enriching textual descriptions. 3) **Supporting various tasks**: M<sup>3</sup>-20M can support model training and tuning for various downstream drug design and discovery tasks, including molecule generation, molecular property prediction, lead optimization, and virtual screening. It also can aid in tasks such as pharmacokinetics modeling and drug-target interaction prediction. Moreover, we construct seven multimodal sub-datasets, QM9-MM, MOSES-MM, BACE-MM,

BBBP-MM, HIV-MM, ClinTox-MM, and Tox21-MM, to facilitate more accurate and robust molecular property prediction.

To demonstrate the power of M<sup>3</sup>-20M in supporting drug design and discovery, extensive experiments on two basic tasks, molecule generation and molecular property prediction, are conducted using large language models including GLM4,<sup>31</sup> GPT-3.5,<sup>32</sup> and GPT-4.<sup>33</sup> The experimental results show that M<sup>3</sup>-20M can significantly boost model performance in both tasks. Concretely, with M<sup>3</sup>-20M, the above models can generate more diverse and valid molecular structures, and achieve higher property prediction accuracy than with existing single-modal datasets, thus verifying the value and potential of M<sup>3</sup>-20M in supporting AI-driven drug design and discovery.


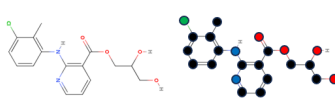
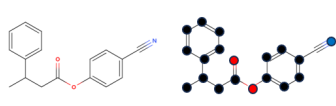
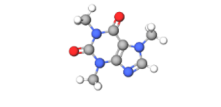
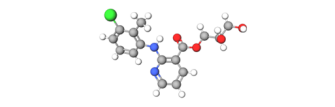
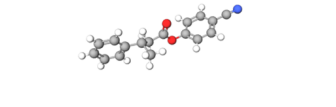

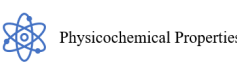
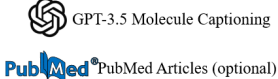
PubChem CID	2519	30823	None
SMILES	<chem>C1(C2=C(N(C(N1C)=O)C)N=C[N]2C)=O</chem>	<chem>Cc1c(Cl)cccc1Nc1ccc(C(=O)OCC(O)CO</chem>	<chem>CC(CC(=O)O)c1ccc(C#N)cc1c1ccccc1</chem>
2D Image/ Graph			
3D Structure			
Pubchem Physicochemical Properties	<b>Molecular Weight</b> 194.19 g/mol <b>XLogP3</b> -0.1 ... <b>Compound Is Canonicalized</b> yes	<b>Molecular Weight</b> 336.77 g/mol <b>XLogP3</b> 2.8 ... <b>Compound Is Canonicalized</b> yes	None
Description Texts	Caffeine appears as odorless white powder or white glistening needles, usually melted together. Bitter taste. Solutions in water are neutral to litmus.	CID is 30823, Compound Name is Clonixetil, Molecular Weight is 336.77, XLogP3 is 2.8, Hydrogen Bond Donor Count is 0, Hydrogen Bond Acceptor Count is 6, Rotatable Bond Count is 7, Exact Mass is 336.0876847, Monoisotopic Mass is 336.0876847...	The molecule is an ester derivative. It contains a benzene ring with an ester group (CC(=O)O) attached to an alkyl chain. The molecule also features an additional phenyl ring with a cyano group (C#N) attached.
Description Source			

Figure 1: Some examples from our M<sup>3</sup>-20M dataset.

## Related Work

Multi-modal molecular data is becoming increasingly important in artificial intelligence and molecular biology. which can provide more comprehensive and rich information, bringing

new opportunities and challenges to drug discovery, molecular property prediction, and generation tasks. For example, Wang et al.<sup>34</sup> pointed out that the use of multi-modal data, including sequence, structure, text etc., can improve the accuracy of drug discovery. However, the challenges faced by multi-modal data cannot be ignored, as different data types often necessitate distinct methods for organization, storage and processing as well as learning. Additionally, ensuring data consistency and integrity also poses a critical issue, with various forms of data potentially exhibiting semantic gaps or inconsistencies. Therefore, there is an urgent need to overcome the above issues to create a large-scale multi-modal integrated dataset for model training or tuning in drug design and discovery. In what follows, we briefly review the related work in three perspectives, molecular representation, single and two-modality molecule datasets, and multi-modality molecule datasets.

## Molecular representations

Molecules can be represented by various modalities of information,<sup>35,36</sup> including one-dimensional sequences, two-dimensional graphs or images, three-dimensional structures, and molecular properties as well as textual descriptions. One-dimensional sequences primarily consist of SMILES strings, molecular fingerprints, and algebraic topology-based characterizations. Two-dimensional representations include molecular graphs and images generated using toolkits such as RDKit<sup>37</sup> or Open Babel.<sup>38</sup> Three-dimensional structures are categorized into molecular graphs and grids,<sup>39</sup> containing atomic coordinates that provide detailed spatial information. Molecular textual descriptions offer additional information derived from experiments. Single-modal data is a reduction of the complete structural information of the molecules, which means the representations learned from single-modal suffer from information loss. For example, two SMILES may represent the same molecule or a two-dimensional molecular graph cannot distinguish between the conformations. Therefore, integrating multi-modal information is crucial for molecular modeling and model training in drug design and discovery.

## Single-modal and two-modal molecule datasets

Most existing molecule datasets are limited to single or dual modalities, restricting the generalization power of trained models.<sup>40–44</sup> These datasets typically have only one-dimensional (1D) SMILES strings, or two-dimensional (2D) structures, or three-dimensional (3D) structures, and usually lack textual molecular descriptions. For instance, MOSES<sup>45</sup> comprises 4,591,276 molecules filtered by molecular weight, ranging from 250 to 350 Daltons, and contains solely one-dimensional SMILES representations. Similarly, ZINC,<sup>46</sup> which serves as a repository of commercially available compounds for virtual screening, contains over 1.3 billion molecules obtained from 310 catalogs across 150 vendors, encompassing 2D graphs and, for the majority, 3D structures. Zeng et al.<sup>29</sup> presented a deep learning system that connects molecular structures with biomedical texts, demonstrating a level of comprehension comparable to that of human experts.

## Multi-modal molecule datasets

With the development of AI-driven drug design and discovery, multi-modal data have become increasingly important in recent years. Up to now, only a few datasets have been introduced to address this need, each with distinct purposes and contributions.

Liu et al.<sup>28</sup> constructed PubChemSTM, a dataset containing over 280,000 chemical structure–text pairs. Despite PubChemSTM’s ability to generalize novel biochemical concepts across various benchmarks, its dataset volume remains insufficient. Subsequently, the igcdata dataset<sup>23</sup> was proposed, which comprises 220,000 descriptions sourced from PubChem and ChEBI-20.<sup>47</sup> Although these two datasets provide valuable resources, their relatively small scale restricts their utility for training high-performance models. Beyond scale, these two datasets also lack the diversity and completeness of molecular modalities necessary for robust model development. Issues such as sparse or overly brief textual descriptions further exacerbate this limitation, leading to suboptimal training outcomes of drug design and discovery models.

To address the limitations of existing datasets and support the training or tuning of high-performance models for drug design and discovery, we present the M<sup>3</sup>-20M dataset, which significantly expands the scale and scope of multi-modal molecular data. Table 1 offers a qualitative comparison of our dataset against existing multi-modal datasets across seven dimensions, including the number of molecules contained, whether consisting of 3D structures, 2D graphs, PubChem CID, physicochemical properties and downstream task datasets, and the number of description texts. From Table 1, we can see that our dataset M<sup>3</sup>-20M has the largest number of molecules and covers the most comprehensive molecular data modalities.

Table 1: Comparison between our dataset M<sup>3</sup>-20M and existing multi-modal datasets.

Property	QM9 <sup>48</sup>	PCdes <sup>29</sup>	PubChemSTM <sup>28</sup>	igcdata <sup>23</sup>	M <sup>3</sup> -20M (Ours)
<b>SMILES</b>	134K	1.5K	280K	220K	20M
<b>3D structures</b>	✓	×	×	×	✓
<b>2D graphs</b>	×	×	✓	×	✓
<b>2D images</b>	×	×	×	✓	✓
<b>PubChem CID</b>	×	×	✓	×	✓
<b>Physicochemical properties</b>	×	×	×	×	✓
<b>Downstream task datasets</b>	×	×	×	×	✓
<b>#Text descriptions</b>	×	1.5K	280K	220K	20M

## Dataset Construction

This section introduces the dataset construction process and some statistic information of the dataset. Molecular data is collected from existing databases PubChem, ZINC and QM9, and then processed to get multiple representations of molecules, including SMILES strings, 2D and 3D structures, physicochemical properties, and textual descriptions. Notably, we enhance

molecular textual descriptions by generating using GPT-3.5 with an expert scoring mechanism to ensure that these descriptions are both scientifically accurate and practically useful. All the data are integrated into a comprehensive dataset with over 20 million molecules.

**Multi-Modal Molecular Dataset Construction**

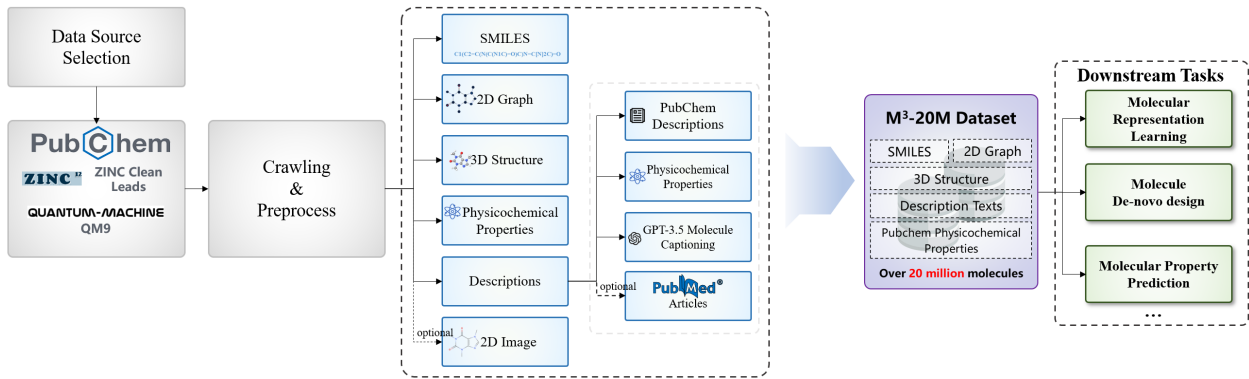


Figure 2: The construction pipeline of our multi-modal molecular dataset M<sup>3</sup>-20M.

## Data Collection

Figure 2 shows the pipeline for constructing our multi-modal molecular dataset M<sup>3</sup>-20M. To obtain molecules and the corresponding molecular graphs and 3D structures, we first collect molecules from the PubChem, ZINC, and QM9 databases for their extensive molecular coverage and reliable data quality. Then, we utilize the Chem function of RDKit to extract atomic features and chemical bond characteristics and convert them into 2D molecular graphs. Additionally, we employ the PubChem API to batch download SDF files containing the 3D structures of molecules and use the GetAtomPosition function of RDKit to calculate the 3D coordinates of the central atoms.

Textual descriptions serve as a bridge for large language models to comprehend multi-modal molecules. The remarkable recognition accuracy and robustness of the CLIP<sup>49</sup> model exemplify the benefits of effectively linking textual descriptions with other modality information of molecules. Similarly, since textual descriptions of molecules facilitate a deeper understanding of chemical information, we meticulously construct these descriptions in the dataset using three approaches: 1) For the molecules that have textual descriptions in



PubChem, we directly extract the texts from PubChem. 2) For the molecules that do not have textual descriptions but have physicochemical properties in PubChem, we transform these physicochemical property values into textual descriptions, which will be detailed later. 3) For those without physicochemical property values or not present in the PubChem database, we generate their textual descriptions by GPT-3.5. We present the details in the following sections.

Initially, we utilized textual data from PubChem; however, only a subset of molecules in PubChem contains associated textual descriptions. The sparsity of text information leads to poor performance of the trained or tuned models. So we resort to text augmentation. To generate textual descriptions for molecules having physicochemical property values in PubChem, we extract 26 key physicochemical properties and their values from PubChem, including Molecular Weight, XLogP3, Hydrogen Bond Donor Count, Hydrogen Bond Acceptor Count, Rotatable Bond Count, Exact Mass, Monoisotopic Mass, Topological Polar Surface Area, Heavy Atom Count, Formal Charge, Complexity, Isotope Atom Count, Defined Atom Stereocenter Count, Undefined Atom Stereocenter Count, Defined Bond Stereocenter Count, Undefined Bond Stereocenter Count, Covalently-Bonded Unit Count, Canonicalization Status, Physical Description, Color/Form, Odor, Boiling Point, Melting Point, Flash Point, and Solubility Density.

Concretely, we search for these properties using the compound identifier (CID) in PubChem, ensuring all data complied with licensing requirements and utilizing the open interface provided by PubChem. After collecting 19,175,245 pieces of raw data, we transform the properties of each molecule into structured descriptions using the template “*property name* is a *specific value*”. Here, “*property name*” indicates any of the 26 properties, and “*specific value*” means a concrete value of the property.

Furthermore, we expand seven downstream task datasets with multi-modal information from our dataset by associating the PubChem CIDs of molecules, including molecule generation datasets MOSES and QM9, and molecular property prediction datasets such as BBBP, BACE,

HIV, Tox21, and ClinTox. This expansion enables model enhancement with multi-modal information for both molecule generation and property prediction tasks. The expanded datasets are denoted as MOSES-MM, QM9-MM, BBBP-MM, BACE-MM, HIV-MM, Tox21-MM, and ClinTox-MM, respectively.

## Text Description Generation by GPT-3.5

As mentioned above, for molecules lacking physicochemical properties or not present in PubChem, we generate molecular textual descriptions as a molecule captioning task by using the GPT-3.5 API. Figure 3 illustrates the process of molecular description text generation. Initially, we use the following prompt to guide GPT-3.5 in generating descriptions based solely on SMILES strings: “*You are an expert chemist. Given the molecular SMILES, your task is to provide a detailed description of the molecule using your experienced chemical knowledge.*”

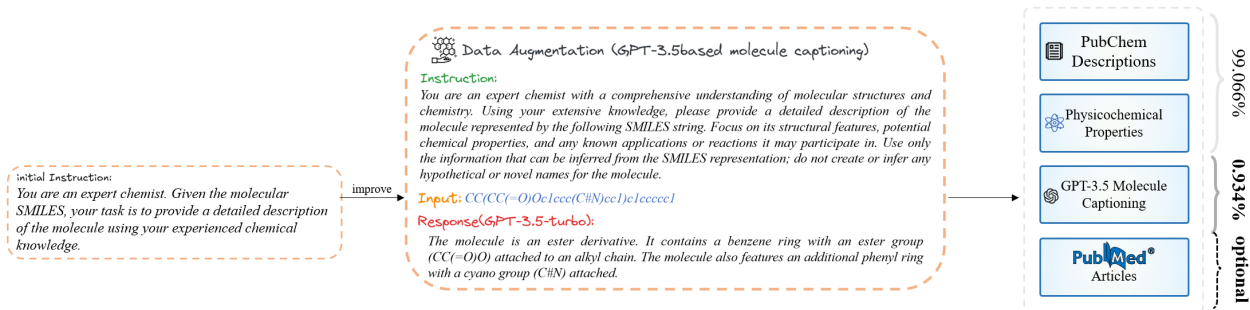


Figure 3: Molecular text description generation by GPT-3.5.

However, this approach results in issues such as incorrect naming of SMILES strings and misidentifying functional groups. To address these problems, inspired by the CO-STAR (Context-Objective-Style-Tone-Audience-Response) framework, we rewrite the original prompt as follows to enhance the output quality: “*You are an expert chemist with a comprehensive understanding of molecular structures and chemistry. Using your extensive knowledge, please describe the molecule represented by the following SMILES string. Focus on its structural features, potential chemical properties, and any known applications or reactions it may participate in. Use only the information inferred from the SMILES representation; do not*

*create or infer any hypothetical or novel names for the molecule.”*

Utilizing this enhanced prompt, we generated 1,073,845 descriptions using GPT-3.5, which is only 0.934% of the total descriptions. The proportion of synthetic data to real data is very low and will not have a negative impact on real data. The following section elaborates on the quality control measures implemented through the Human Expert Scoring Mechanism to ensure the precision and reliability of the generated descriptions.

## Generated Text Quality Control by Human Expert Scoring

To ensure the reliability and utility of the generated textual descriptions, we implement an expert scoring mechanism inspired by some recent works.<sup>50,51</sup> We recruit six undergraduate and postgraduate chemistry students from top China universities, all having excellent academic records. They evaluate the accuracy and usefulness of the generated texts, ensuring that the textual descriptions are both scientifically valid and practically useful.

This mechanism assesses the textual descriptions from four dimensions: *accuracy*, *effectiveness*, *comprehensiveness*, and *simplicity*, as established in previous works on natural language generation and evaluation.<sup>52,53</sup> Each description can earn a maximum score of 10 points. The scoring system is structured as follows:

### 1. Accuracy (Maximum 5 points)

- (a) **Correct Description (5 points):** The molecular description is entirely accurate, containing no scientific errors. This includes correct usage of chemical terms, accurate structural representation, and proper property identification.
- (b) **Slight Errors (2-4 points):** Minor inaccuracies are present, such as small structural mistakes or minor property deviations. These errors should not impede overall comprehension. Notably, any incorrect identification of functional groups results in a 1 point deduction.
- (c) **Serious Errors (0 points):** Major inaccuracies are present, such as entirely

incorrect chemical terminology or wrong molecular names, stripping the description of scientific value.

## 2. Effectiveness (Maximum 2 points)

- (a) **Highly Valid (2 points):** The description highlights key molecular properties, such as reactivity or pharmacodynamics, and may include useful applications or future prospects.
- (b) **Moderately Effective (1 point):** While the description includes valid information, it may lack detailed analysis or specific application scenarios.
- (c) **Ineffective Description (0 points):** The description fails to convey crucial properties or applications and lacks practical utility.

## 3. Comprehensiveness (Maximum 2 points)

- (a) **Very Comprehensive (2 points):** The description extensively covers multiple aspects of the molecule, including structure, physicochemical properties, reactivity, and potential applications.
- (b) **Fairly Comprehensive (1 point):** Several aspects of the molecule are described, though some areas may lack depth.
- (c) **Incomplete (0 points):** The description is limited to one aspect of the molecule and significantly lacks breadth.

## 4. Simplicity (Maximum 1 point)

- (a) **Concise (1 point):** Succinct, clearly articulated, and free of redundant information.
- (b) **Not Concise (0 points):** Verbose and repetitive, detracting from clarity and conciseness.

Each text description is evaluated based on a maximum score of 10 points. For every 100 generated molecules, 10% are randomly selected for expert scoring. Descriptions scoring above 5 points are considered qualified, while those below 5 points are regenerated. Descriptions with significant inaccuracies (0 points in accuracy) will also be regenerated.

## Statistic Results

This section presents some statistic information of the M<sup>3</sup>-20M dataset to highlight its comprehensive annotations, diverse textual descriptions and physicochemical properties, which can significantly enhance its utility for molecular research and AI-driven drug discovery. By comparing it with existing datasets such as PubChem, we emphasize the enhancements in both scale and quality that M<sup>3</sup>-20M offers. The section further delves into word distribution — a key feature of textual data, and explores correlations among physicochemical properties through advanced statistical techniques like Principal Component Analysis (PCA). Additionally, we outline the robust maintenance protocols established to ensure our dataset’s accuracy and usability for the research community. These findings demonstrate the dataset’s value as a fundamental resource for molecular representation learning and related applications.

## Textual Descriptions

Figure 4 shows a comparison of molecule descriptions between PubChem and our M<sup>3</sup>-20M. The PubChem description bar is relatively small, reaching only 360,133, while the M<sup>3</sup>-20M annotation description bar towers over it, marking a count of 20,249,090. This enhancement is critical for AI-driven drug design and discovery, as the increased volume and details of descriptions facilitate more comprehensive analysis and model training.

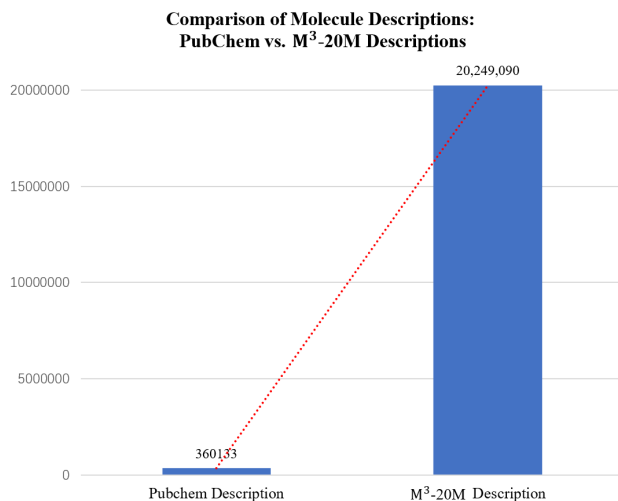


Figure 4: Comparison of molecule descriptions: PubChem vs. our M<sup>3</sup>-20M

## Word Distribution in Description Texts

Figure 5 presents the top 20 most frequently occurring words in the textual descriptions of our dataset, plotted alongside their respective frequencies to emphasize their relative prominence. The most commonly used terms, such as 'natural,' 'product,' and 'acid,' appear tens of thousands of times, underscoring their central role in describing molecular properties and functions. Additional notable terms, including 'related,' 'organisms,' and 'amino,' further highlight the biological and chemical contexts associated with these molecules. This visualization of word frequencies provides valuable insights into molecular datasets' linguistic patterns and descriptive focus.

## Physicochemical Properties

Table 2 and Figure 6 provide a detailed overview of the specific names, corresponding quantities, and reference of the 26 key physicochemical properties extracted from PubChem. Of the 26 key physicochemical properties, 18 are computed using professional software <sup>1</sup>, while the remaining 8 represent experimental values sourced from the CAMEO Chemicals database and Hazardous Substances Data Bank (HSDB). Notably, 18 of these properties

<sup>1</sup>PubChem 2.2; Cactvs 3.4.8.18

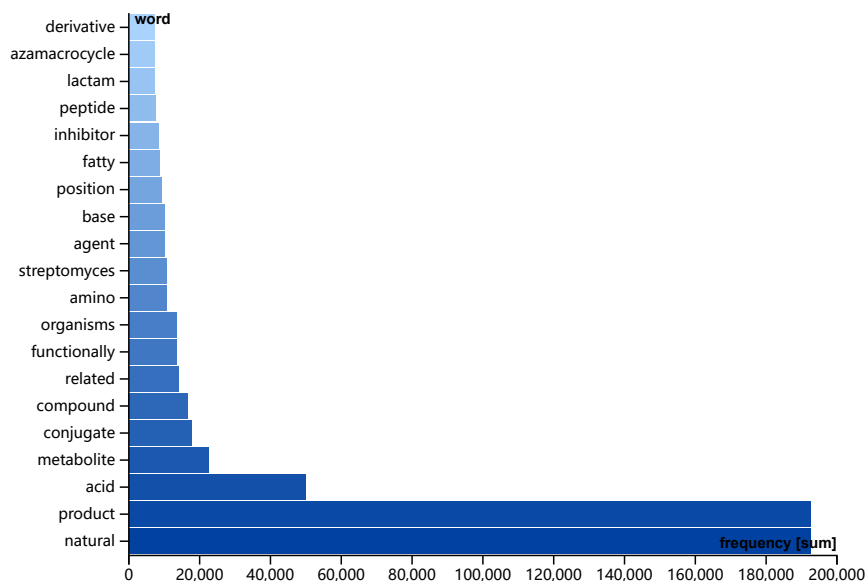


Figure 5: Top 20 most frequent words in textual descriptions.

exhibit quantities reaching tens of millions, underscoring our dataset’s extensive coverage and comprehensiveness.

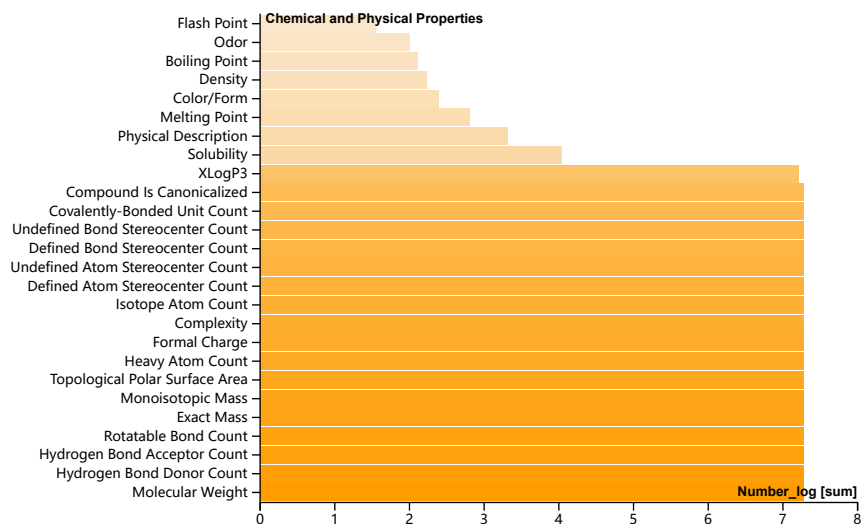


Figure 6: Physicochemical property distribution.

As shown in Figure 7, we first calculate the correlation matrix of all physicochemical properties and draw a heat map. We find that Molecular Weight and XLogP3 are the most suitable because they exhibit strong correlations with several other key properties, indicating

Table 2: The 26 key physicochemical properties and their corresponding numbers and references.

Physicochemical Properties	Number	Reference
Molecular Weight	19174000	Computed by PubChem 2.2
XLogP3	16340203	Computed by XLogP3 3.0
Hydrogen Bond Donor Count	19173687	Computed by Cactvs 3.4.8.18
Hydrogen Bond Acceptor Count	19173559	Computed by Cactvs 3.4.8.18
Rotatable Bond Count	19173464	Computed by Cactvs 3.4.8.18
Exact Mass	19173398	Computed by PubChem 2.2
Monoisotopic Mass	19173327	Computed by PubChem 2.2
Topological Polar Surface Area	19173287	Computed by Cactvs 3.4.8.18
Heavy Atom Count	19173259	Computed by PubChem
Formal Charge	19173222	Computed by PubChem
Complexity	19173210	Computed by Cactvs 3.4.8.18
Isotope Atom Count	19173193	Computed by PubChem
Defined Atom Stereocenter Count	19173170	Computed by PubChem
Undefined Atom Stereocenter Count	19173153	Computed by PubChem
Defined Bond Stereocenter Count	19173147	Computed by PubChem
Undefined Bond Stereocenter Count	19173137	Computed by PubChem
Covalently-Bonded Unit Count	19173132	Computed by PubChem
Compound Is Canonicalized	19173130	Computed by PubChem
Physical Description	2031	CAMEO Chemicals database
Color/Form	246	Hazardous Substances Data Bank (HSDB)
Odor	100	Hazardous Substances Data Bank (HSDB)
Boiling Point	130	CAMEO Chemicals database
Melting Point	633	CAMEO Chemicals database
Flash Point	35	CAMEO Chemicals database
Solubility	10813	CAMEO Chemicals database
Density	170	CAMEO Chemicals database

their ability to capture significant variance in the dataset. Thus, we select these two properties as the first and second principal components for Principal Components Analysis (PCA) and visualize the molecular space of randomly sampled 10000 molecules as shown in Figure 8.

## Dataset Maintenance

To ensure the accessibility and accuracy of the M<sup>3</sup>-20M dataset, we have organized a dedicated maintenance team consisting of six members, including three doctoral students and three master’s students. This team will perform regular maintenance twice a week, correcting any errors and updating the dataset as needed. This rigorous maintenance protocol supports the community’s exploration of molecular representation and downstream molecular tasks and facilitates the training of large models with improved versatility and robustness.

## Supporting Various Downstream Tasks

The M<sup>3</sup>-20M dataset supports model training and tuning for various downstream drug design and discovery tasks. While general large language models have achieved remarkable success in natural language processing, their performance in specialized fields like drug design and



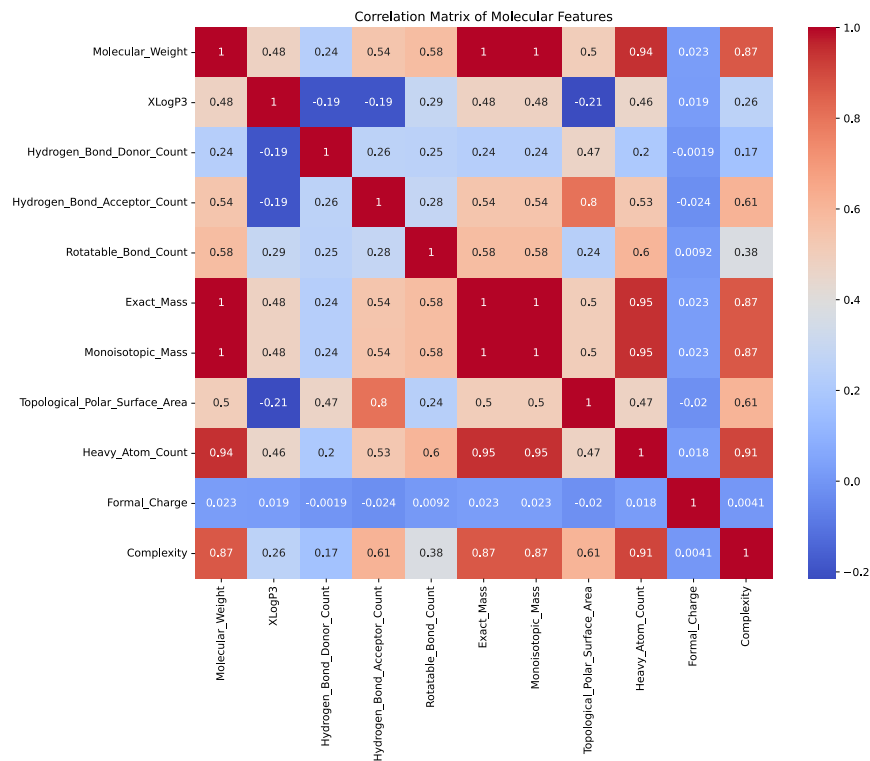


Figure 7: Correlation matrix of physicochemical properties.

discovery still has significant room for improvement. Figure 9 illustrates how to use the M<sup>3</sup>-20M dataset to enhance large language models (LLMs) or train models for downstream drug design and discovery tasks, which consists of three paradigms: prompting, finetuning, and training from scratch.

Prompt engineering involves carefully constructing input prompts to guide a general large language model (LLM) in generating more accurate outputs tailored to drug design and discovery. By leveraging our M<sup>3</sup>-20M dataset, prompt engineering allows the model to quickly adapt to this field without altering its internal parameters. Fine-tuning refers to further training the LLMs on the M<sup>3</sup>-20M dataset, adjusting certain model parameters based on existing pre-training. This process enables the model to better align with the specific characteristics and needs of drug design and discovery while retaining its general language knowledge. Training from scratch entails building and training a language model on drug design and discovery domain data. This approach necessitates a large volume of training

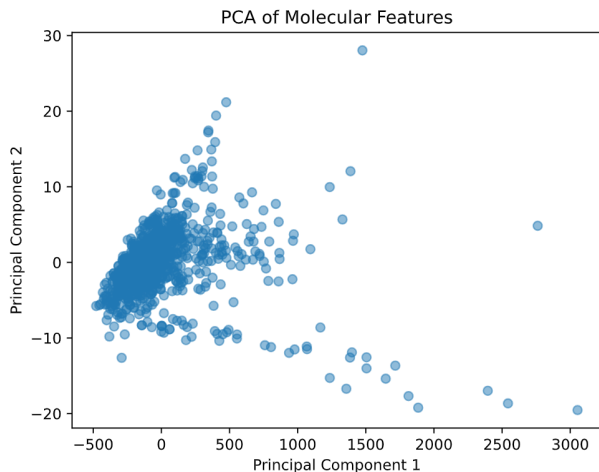


Figure 8: Visualization of molecular space with principal component analysis (PCA).

data, which our M<sup>3</sup>-20M dataset can adequately provide. By utilizing our M<sup>3</sup>-20M dataset through prompt engineering, fine-tuning, and training from scratch, the general LLM’s drug design and discovery capabilities can be enhanced from multiple perspectives and to varying degrees.

M<sup>3</sup>-20M also can aid in tasks such as pharmacokinetics modeling and drug-target interaction prediction. Moreover, we construct seven multimodal sub-datasets, QM9-MM, MOSES-MM, BACE-MM, BBBP-MM, HIV-MM, ClinTox-MM, and Tox21-MM, to facilitate more accurate and robust molecular property prediction. We also provide tools for generating molecular images to support compound patent searches and for crawling PubMed to find articles related to specific molecules, thereby enhancing textual descriptions.

## Dataset Evaluation

In this section, we evaluate the effectiveness of the M<sup>3</sup>-20M dataset on two fundamental downstream tasks: molecule generation and molecular property prediction. We primarily perform prompt tuning and in-context learning on the closed-source large language models GLM4, GPT-3.5, and GPT-4, while also conducting fine-tuning on the open-source model Llama3-8b. Additionally, our dataset can be applied to other tasks, including name prediction,

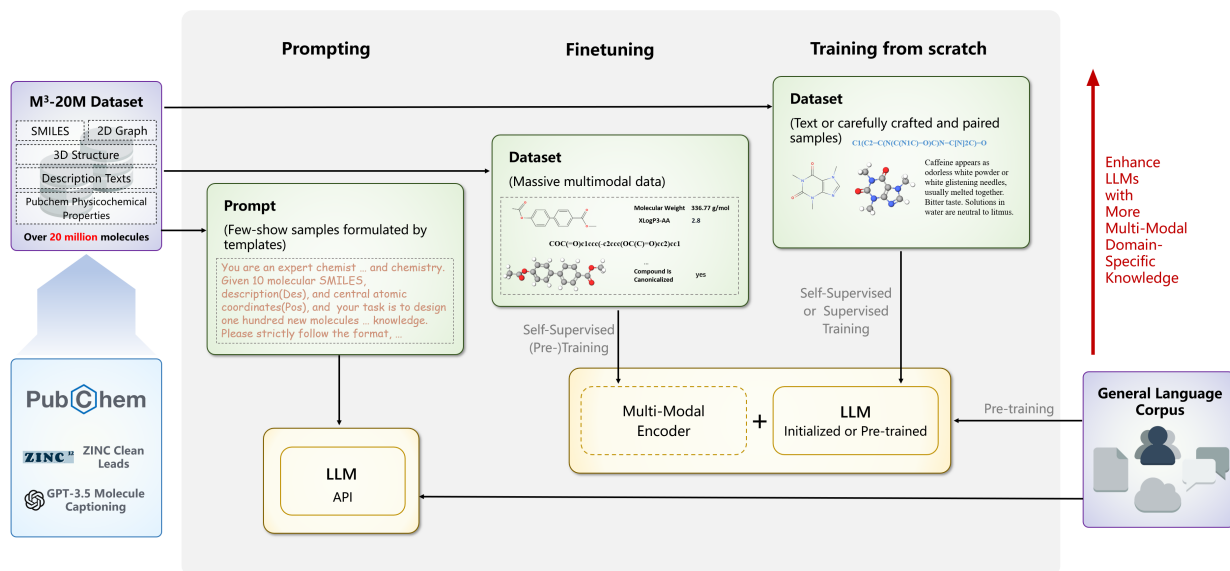


Figure 9: Paradigms of model training and finetuning using our dataset.

reaction prediction, retrosynthesis, text-based molecule design, and molecule captioning. Our findings demonstrate that M<sup>3</sup>-20M significantly enhances model performance across these molecular tasks.

## Molecule Generation

We utilize the GLM-4, GPT-3.5, and GPT-4 APIs to evaluate the power of M<sup>3</sup>-20M in molecule generation. Through in-context learning (ICL),<sup>54</sup> we provide 10 randomly selected multi-modal examples (including SMILES strings of molecules, three-dimensional atomic coordinates, and descriptions) and single-modal examples (containing only SMILES), respectively. Subsequently, 100 molecules are generated randomly for each setup.

We analyze the performance of models trained on single-modal and multi-modal datasets in molecule generation using three metrics: *validity*, *uniqueness*, and *novelty*. The results, presented in Table 3, demonstrate the superiority of multi-modal datasets across all metrics and models.

**Validity** measures the proportion of chemically valid generated molecules. Multi-modal datasets consistently outperform single-modal ones. For instance, GLM4’s validity improves

from 72.73% to 85.37%, GPT-3.5’s from 76.01% to 84.8%, and GPT-4’s from 92.3% to 97.99%.

**Uniqueness** assesses the diversity of generated molecules. Multi-modal datasets show significant improvements: GLM4’s uniqueness rises from 68.17% to 82.25%, GPT-3.5’s from 46.46% to 93.86%, and GPT-4’s from 58.64% to 70.17%.

**Novelty** evaluates the proportion of generated novel molecules. Multi-modal datasets show substantial improvements, with GLM4’s novelty increasing from 97.90% to 98.10%, GPT-3.5’s from 85.72% to 96.51%, and GPT-4’s from 90.66% to 98.95%.

Table 3: Molecule generation performance comparison: multi-modal data vs. single-modal data.

	Validity(%) $\uparrow$		Uniqueness(%) $\uparrow$		Novelty(%) $\uparrow$	
	Single-modal	Multi-modal	Single-modal	Multi-modal	Single-modal	Multi-modal
GLM4	72.73( $\pm$ 1.73)	<b>85.37</b> ( $\pm$ 1.58)	68.17( $\pm$ 2.94)	<b>82.25</b> ( $\pm$ 2.95)	97.90( $\pm$ 0.98)	<b>98.10</b> ( $\pm$ 1.23)
GPT-3.5	76.01( $\pm$ 5.63)	<b>84.8</b> ( $\pm$ 0.6)	46.46( $\pm$ 3.23)	<b>93.86</b> ( $\pm$ 1.49)	85.72( $\pm$ 0.67)	<b>96.51</b> ( $\pm$ 1.57)
GPT-4	92.3( $\pm$ 3.85)	<b>97.99</b> ( $\pm$ 0.41)	58.64( $\pm$ 0.36)	<b>70.17</b> ( $\pm$ 4.92)	90.66( $\pm$ 1.14)	<b>98.95</b> ( $\pm$ 0.34)

Furthermore, Table 4 summarizes the molecular generation performance of our M<sup>3</sup>-20M dataset using MOSES-MM as the benchmark. Multi-modal data enhances SNN/Test performance for GPT-3.5 and GPT-4, showing increased similarity to the test set. For Frag/Test, multi-modal data boosts GLM4 to 0.27% and GPT-4 to 0.20%. In Scaf/Test, all models improve with multi-modal data; GLM4 rises to 0.07%, while GPT-3.5 and GPT-4 each improve to 0.01%. Regarding Filters, GLM4’s pass rate increases to 0.80% with multi-modal data, while GPT-3.5 maintains 1.0%.

Metrics like logP, SA, QED, and molecular weight are assessed using the Wasserstein-1 distance to the MOSES-MM test set, where lower values indicate better performance. Multi-modal data significantly reduces logP distance, especially for GPT-3.5 (0.99) and GPT-4 (0.92), indicating superior predictions. In SA, multi-modal data improves scores for GPT-3.5 and GPT-4, reducing distances to 0.57 and 0.54, respectively. QED scores improve with multi-modal data, reaching 0.12 for both models. For molecular weight, predictions improve for GLM4, reducing the distance to 105.72.

These findings demonstrate that our multi-modal dataset significantly enhances molecule generation models across nearly all metrics, highlighting the benefit of integrating diverse molecular representations. The results support the widespread use of multi-modal data in molecular research to develop more robust and versatile generative models.

Table 4: Molecule generation performance comparison on MOSES-MM.

		GLM4	GPT-3.5	GPT-4
SNN/Test(%) $\uparrow$	Single-modal	0.49( $\pm$ 0.03)	0.53( $\pm$ 0.09)	0.49( $\pm$ 0.07)
	Multi-modal	0.44( $\pm$ 0.09)	<b>0.56</b> ( $\pm$ 0.04)	<b>0.52</b> ( $\pm$ 0.01)
Frag/Test(%) $\uparrow$	Single-modal	0.24( $\pm$ 0.02)	0.44( $\pm$ 0.12)	0.19( $\pm$ 0.08)
	Multi-modal	<b>0.27</b> ( $\pm$ 0.14)	0.32( $\pm$ 0.01)	<b>0.20</b> ( $\pm$ 0.01)
Scaf/Test(%) $\uparrow$	Single-modal	0.04( $\pm$ 0.05)	6.90e-4( $\pm$ 6.90e-4)	2.01e-3( $\pm$ 4.13e-4)
	Multi-modal	<b>0.07</b> ( $\pm$ 0.09)	<b>0.01</b> ( $\pm$ 0.01)	<b>0.01</b> ( $\pm$ 4.99e-3)
Filters(%) $\uparrow$	Single-modal	0.73( $\pm$ 0.09)	0.8( $\pm$ 0.0)	1.0( $\pm$ 0.0)
	Multi-modal	<b>0.80</b> ( $\pm$ 1.11e-16)	<b>1.0</b> ( $\pm$ 0.0)	0.9( $\pm$ 0.10)
logP( $\downarrow$ )	Single-modal	1.35( $\pm$ 0.17)	1.63( $\pm$ 0.32)	1.27( $\pm$ 0.31)
	Multi-modal	1.44( $\pm$ 0.28)	<b>0.99</b> ( $\pm$ 0.05)	<b>0.92</b> ( $\pm$ 0.11)
SA( $\downarrow$ )	Single-modal	0.83( $\pm$ 0.22)	0.63( $\pm$ 0.11)	0.60( $\pm$ 0.14)
	Multi-modal	1.00( $\pm$ 0.10)	<b>0.57</b> ( $\pm$ 0.02)	<b>0.54</b> ( $\pm$ 0.06)
QED( $\downarrow$ )	Single-modal	0.20( $\pm$ 0.04)	0.15( $\pm$ 0.05)	0.15( $\pm$ 0.06)
	Multi-modal	0.20( $\pm$ 0.08)	<b>0.12</b> ( $\pm$ 0.03)	<b>0.12</b> ( $\pm$ 0.02)
weight( $\downarrow$ )	Single-modal	112.10( $\pm$ 20.66)	67.83( $\pm$ 15.92)	89.75( $\pm$ 37.98)
	Multi-modal	<b>105.72</b> ( $\pm$ 38.35)	68.01( $\pm$ 4.04)	95.62( $\pm$ 9.33)

Table 5: Model performance comparison among different datasets.

Datasets	Validity(%) $\uparrow$	Uniqueness(%) $\uparrow$	Novelty(%) $\uparrow$
QM9 <sup>48</sup>	75.17 ( $\pm$ 1.43)	64.13 ( $\pm$ 1.58)	89.43 ( $\pm$ 0.01)
Pcdes <sup>29</sup>	84.31 ( $\pm$ 0.24)	82.64 ( $\pm$ 1.60)	93.253 ( $\pm$ 0.59)
PubChemSTM <sup>28</sup>	82.24 ( $\pm$ 0.70)	80.89 ( $\pm$ 1.12)	95.91 ( $\pm$ 1.93)
igcdata <sup>23</sup>	78.34 ( $\pm$ 2.22)	61.21 ( $\pm$ 1.50)	95.07 ( $\pm$ 0.07)
Ours	<b>84.8</b> ( $\pm$ 0.6)	<b>93.86</b> ( $\pm$ 1.49)	<b>96.51</b> ( $\pm$ 1.57)

Finally, we compare the molecule generation performance of GPT-3.5 across various datasets: QM9, Pcdes, PubChemSTM, igcdata, and our M<sup>3</sup>-20M, focusing on Validity, Uniqueness, and Novelty. Table 5 presents the experimental results.

Using our dataset, the model achieves the highest validity score of 84.8%, surpassing all other datasets, indicating the effectiveness of M<sup>3</sup>-20M in generating chemically accurate molecules. For uniqueness, our dataset again leads with 93.86%, significantly higher than Pcdes and PubChemSTM, demonstrating its capacity to support the generation of diverse molecular structures essential for discovering novel compounds. Our dataset also achieves the highest novelty score of 96.51%, followed by PubChemSTM at 95.91% and Pcdes at 93.25%, underscoring its effectiveness in generating unique molecular structures.

Overall, the comparison across Validity, Uniqueness, and Novelty highlights the superiority of our M<sup>3</sup>-20M dataset. It enables the generation of chemically valid molecules with high diversity and novelty, making it a valuable resource for model training and tuning in drug design and discovery.

## Molecular Property Prediction

We refer to MoleculeNet<sup>4</sup> and divide the molecular property prediction task into regression task and classification task.

**Regression tasks:** To test the effectiveness of our multi-modal dataset in support of molecule property prediction tasks, we conduct an ablation experiment on the QM9-MM dataset with three settings: using only the SMILES strings of molecules; using both the SMILES strings and 3D coordinates of molecules; and using the SMILES strings, 3D coordinates and the textual descriptions of molecules. We consider two regression tasks: predicting the dipole moment ( $\mu$ ) and isotropic polarizability ( $\alpha$ ) of the given molecules. We employ GPT-3.5, GPT-4, and GLM-4 APIs to infer the molecular properties respectively. For each molecule to be inferred, we provide the corresponding molecule information in the prompt based on the different versions of the settings and randomly select four additional molecule examples to help the LLMs better understand the chemical structure and the relation between the molecule information and the prediction ground truth.

The metric we use for the regression tasks is Mean Absolute Error (MAE), measuring the average magnitude of errors between predicted values and actual values. The smaller the MAE value, the more accurate the prediction. The formula of the MAE metric is as follows:

$$\text{MAE} = \frac{1}{n} \sum_{i=1}^n |y_i - \hat{y}_i| \quad (1)$$

while  $n$  is the number of samples,  $y_i$  is predicted value, and  $\hat{y}_i$  is the ground truth value.

The results in Table 6 show that providing more information with multi-modal data in the prompt can help LLMs better understand molecules and their chemical properties. Except for the task of predicting the dipole moment using GPT-4, all other models and tasks achieve the best results on the multi-modal dataset, which proves the effectiveness and high quality of our dataset.

Table 6: Performance comparison of models using different modal data.

	SMILES		SMILES+3D		SMILES+3D+texts	
	$\mu$	$\alpha$	$\mu$	$\alpha$	$\mu$	$\alpha$
GPT-3.5	1.78 ( $\pm 0.16$ )	39.50 ( $\pm 2.16$ )	1.82 ( $\pm 0.36$ )	35.37 ( $\pm 1.53$ )	<b>1.56</b> ( $\pm 0.28$ )	<b>34.74</b> ( $\pm 1.60$ )
GLM-4	1.27 ( $\pm 0.13$ )	12.82 ( $\pm 0.77$ )	1.13 ( $\pm 0.07$ )	14.53 ( $\pm 0.67$ )	<b>1.01</b> ( $\pm 0.13$ )	<b>12.05</b> ( $\pm 0.48$ )
GPT-4	<b>1.17</b> ( $\pm 0.12$ )	13.71 ( $\pm 0.08$ )	1.28 ( $\pm 0.20$ )	28.9 ( $\pm 0.84$ )	1.27 ( $\pm 0.30$ )	<b>9.50</b> ( $\pm 1.65$ )

**Classification tasks:** We evaluate the performance of single-modal and multi-modal datasets on various molecular property prediction tasks, focusing on accuracy mean (ACC Mean), accuracy variance (ACC Variance), and accuracy standard deviation (ACC Standard Deviation). The results are summarized in Table 7.

ACC Mean measures the average accuracy of the models. Multi-modal datasets show improvements over single-modal datasets. For example, the BACE-MM dataset’s ACC Mean increases from 0.5680 to 0.5780, and the BBBP-MM dataset sees an increase from 0.2280 to 0.2720. The ClinTox-MM dataset improves from 0.9260 to 0.9280, while the HIV-MM

dataset shows a higher ACC Mean for single-modal data (0.9740) compared to multi-modal (0.9680). These results suggest that multi-modal datasets typically enhance model accuracy. ACC Variance indicates the variability in accuracy. The ClinTox-MM dataset’s variance decreases from 0.0005 to 0.0002 with multi-modal data, indicating more stable performance. ACC Standard Deviation provides insight into the distribution of accuracy values. The ClinTox-MM dataset sees a reduction from 0.0230 to 0.0130, suggesting enhanced consistency.

Table 7: Accuracy comparison between single-modal and multi-modal datasets for molecular property prediction tasks.

	ACC Mean		ACC Variance		ACC Standard Deviation	
	Single-modal	Multi-modal	Single-modal	Multi-modal	Single-modal	Multi-modal
BACE-MM	0.5680	<b>0.5780</b>	0.0014	0.0018	0.0377	0.0427
BBBP-MM	0.2280	<b>0.2720</b>	0.0005	0.0008	0.0217	0.0277
ClinTox-MM	0.9260	<b>0.9280</b>	0.0005	0.0002	0.0230	0.0130
HIV-MM	<b>0.9740</b>	0.9680	0.0002	0.0002	0.0134	0.0148

We compare the performance of single-modal and multi-modal datasets on various molecular property prediction tasks with the Tox21-MM dataset as the benchmark. The results are summarized in Table 8.

For ACC Mean, multi-modal datasets generally show an improvement. For example, in the NR-AR task, the ACC Mean increases from 0.9620 to 0.9680 with multi-modal data. Similarly, the NR-AhR task shows a rise from 0.8740 to 0.9020, and the NR-Aromatase task improves from 0.9620 to 0.9720. These results suggest that multi-modal datasets generally enhance accuracy. For ACC Variance, both the NR-AR and NR-PPAR-gamma tasks show equal variances of 0.0003 and 0.0002, indicating consistent performance. The NR-ER task significantly reduces variance from 0.0014 to 0.0003 with multi-modal data, highlighting improved stability. For ACC Standard Deviation, the SR-HSE task decreases significantly from 0.0295 to 0.0114 with multi-modal data, suggesting enhanced consistency.

Additionally, fine-tuning Llama3-8b with our data shows notable improvements. Results in Table 9 shows that fine-tuning Llama3-8b with our M<sup>3</sup>-20M dataset leads to notable



Table 8: Accuracy comparison between single-modal and multi-modal datasets on Tox21-MM.

	ACC Mean		ACC Variance		ACC Standard Deviation	
	Single-modal	Multi-modal	Single-modal	Multi-modal	Single-modal	Multi-modal
NR-AR	0.9620	<b>0.9680</b>	0.0003	0.0003	0.0164	0.0164
NR-AR-LBD	0.9800	<b>0.9800</b>	0.0002	0.0003	0.0141	0.0173
NR-AhR	0.8740	<b>0.9020</b>	0.0006	0.0009	0.0251	0.0303
NR-Aromatase	0.9620	<b>0.9720</b>	0.0001	0.0005	0.0110	0.0217
NR-ER	0.9140	<b>0.9240</b>	0.0014	0.0003	0.0378	0.0167
NR-ER-LBD	<b>0.9580</b>	0.9560	0.0003	0.0009	0.0179	0.0297
NR-PPAR-gamma	0.9780	<b>0.9780</b>	0.0002	0.0002	0.0148	0.0148
SR-ARE	<b>0.9060</b>	0.8680	0.0002	0.0005	0.0152	0.0217
SR-ATAD5	<b>0.9680</b>	0.9600	0.0005	0.0003	0.0228	0.0158
SR-HSE	0.9520	<b>0.9560</b>	0.0009	0.0001	0.0295	0.0114
SR-MMP	0.8820	<b>0.8960</b>	0.0008	0.0016	0.0277	0.0404
SR-p53	<b>0.9500</b>	0.9340	0.0005	0.0014	0.0235	0.0378

improvements in model performance across various tasks. Specifically, the multi-modal results show significant gains over the single-modal baseline for the BACE, Tox21, HIV, and ClinTox datasets, with the most pronounced improvement seen on the BACE dataset, where performance increases from 0.844 to 0.887. This proves that our dataset has a wide range of application scenarios and practical value. In fact, our dataset can also be used for downstream tasks such as name prediction, reaction prediction, retrosynthesis, text-based molecule design, molecule captioning etc.

Table 9: Fine-tuning Llama3-8b with our M<sup>3</sup>-20M dataset

Dataset	Single-modal	Multi-modal (ours)
BBBP	0.959	<b>0.959</b>
BACE	0.844	<b>0.887</b>
Tox21	0.817	<b>0.849</b>
HIV	0.780	<b>0.803</b>
ClinTox	0.985	<b>0.998</b>

## Conclusion

In this paper, we introduce M<sup>3</sup>-20M, a new and large-scale multi-modal molecular dataset containing over 20 million molecules. Extensive experiments demonstrate M<sup>3</sup>-20M’s effectiveness in boosting the performance of various models in molecule generation and property prediction. M<sup>3</sup>-20M’s integration of SMILES strings, 2D graphs, 3D structural data, physicochemical properties, and molecular textual descriptions provides a rich foundation for developing high-performance generative models for AI-driven drug design and discovery.

## Acknowledgement

This work was supported in part by the National Natural Science Foundation of China (NO. 62372326, No. 62172300).

## Data and Software Availability Statement

The dataset is openly accessible for non-commercial use, hosted on a publicly available platform (<https://github.com/bz99bz/M-3>). This project also provides detailed dataset documentation and the workflow code discussed in the present paper.

## References

- (1) Santos, R.; Ursu, O.; Gaulton, A.; Bento, A. P.; Donadi, R. S.; Bologa, C. G.; Karlsson, A.; Al-Lazikani, B.; Hersey, A.; Oprea, T. I., et al. A comprehensive map of molecular drug targets. *Nature reviews Drug discovery* **2017**, *16*, 19–34.
- (2) Hughes, J. P.; Rees, S.; Kalindjian, S. B.; Philpott, K. L. Principles of early drug discovery. *British journal of pharmacology* **2011**, *162*, 1239–1249.

- (3) Tsaïoun, K.; Blaauboer, B. J.; Hartung, T. Evidence-based absorption, distribution, metabolism, excretion (ADME) and its interplay with alternative toxicity methods. *ALTEX-Alternatives to animal experimentation* **2016**, *33*, 343–358.
- (4) Wu, Z.; Ramsundar, B.; Feinberg, E. N.; Gomes, J.; Geniesse, C.; Pappu, A. S.; Leswing, K.; Pande, V. MoleculeNet: a benchmark for molecular machine learning. *Chemical science* **2018**, *9*, 513–530.
- (5) Chen, W.; Liu, X.; Zhang, S.; Chen, S. Artificial intelligence for drug discovery: Resources, methods, and applications. *Molecular Therapy-Nucleic Acids* **2023**, *31*, 691–702.
- (6) Ji, K.-Y.; Liu, C.; Liu, Z.-Q.; Deng, Y.-F.; Hou, T.-J.; Cao, D.-S. Comprehensive assessment of nine target prediction web services: which should we choose for target fishing? *Briefings in Bioinformatics* **2023**, *24*, bbad014.
- (7) Ye, Q.; Hsieh, C.-Y.; Yang, Z.; Kang, Y.; Chen, J.; Cao, D.; He, S.; Hou, T. A unified drug–target interaction prediction framework based on knowledge graph and recommendation system. *Nature communications* **2021**, *12*, 6775.
- (8) Li, F.; Zhang, Z.; Guan, J.; Zhou, S. Effective drug–target interaction prediction with mutual interaction neural network. *Bioinformatics* **2022**, *38*, 3582–3589.
- (9) Lu, W.; Zhang, J.; Huang, W.; Zhang, Z.; Jia, X.; Wang, Z.; Shi, L.; Li, C.; Wolynes, P. G.; Zheng, S. DynamicBind: predicting ligand-specific protein-ligand complex structure with a deep equivariant generative model. *Nature Communications* **2024**, *15*, 1071.
- (10) Fu, L.; Shi, S.; Yi, J.; Wang, N.; He, Y.; Wu, Z.; Peng, J.; Deng, Y.; Wang, W.; Wu, C., et al. ADMETlab 3.0: an updated comprehensive online ADMET prediction platform enhanced with broader coverage, improved performance, API functionality and decision support. *Nucleic Acids Research* **2024**, gkae236.

- (11) Goldman, S.; Bradshaw, J.; Xin, J.; Coley, C. Prefix-tree decoding for predicting mass spectra from molecules. *Advances in Neural Information Processing Systems* **2023**, *36*, 48548–48572.
- (12) Rong, Y.; Bian, Y.; Xu, T.; Xie, W.; Wei, Y.; Huang, W.; Huang, J. Self-supervised graph transformer on large-scale molecular data. *Advances in neural information processing systems* **2020**, *33*, 12559–12571.
- (13) Masters, D.; Dean, J.; Klaser, K.; Li, Z.; Maddrell-Mander, S.; Sanders, A.; Helal, H.; Beker, D.; Rampásek, L.; Beaini, D. Gps++: An optimised hybrid mpnn/transformer for molecular property prediction. *arXiv preprint arXiv:2212.02229* **2022**,
- (14) Gao, W.; Fu, T.; Sun, J.; Coley, C. Sample efficiency matters: a benchmark for practical molecular optimization. *Advances in neural information processing systems* **2022**, *35*, 21342–21357.
- (15) Franke, J.; Runge, F.; Hutter, F. Probabilistic transformer: Modelling ambiguities and distributions for rna folding and molecule design. *Advances in Neural Information Processing Systems* **2022**, *35*, 26856–26873.
- (16) Kong, X.; Huang, W.; Tan, Z.; Liu, Y. Molecule generation by principal subgraph mining and assembling. *Advances in Neural Information Processing Systems* **2022**, *35*, 2550–2563.
- (17) Yang, S.; Hwang, D.; Lee, S.; Ryu, S.; Hwang, S. J. Hit and lead discovery with explorative rl and fragment-based molecule generation. *Advances in Neural Information Processing Systems* **2021**, *34*, 7924–7936.
- (18) Song, Y.; Gong, J.; Xu, M.; Cao, Z.; Lan, Y.; Ermon, S.; Zhou, H.; Ma, W.-Y. Equivariant Flow Matching with Hybrid Probability Transport for 3D Molecule Generation. *Advances in Neural Information Processing Systems* **2024**, *36*.

- (19) Bagal, V.; Aggarwal, R.; Vinod, P.; Priyakumar, U. D. MolGPT: molecular generation using a transformer-decoder model. *Journal of Chemical Information and Modeling* **2021**, *62*, 2064–2076.
- (20) Chithrananda, S.; Grand, G.; Ramsundar, B. ChemBERTa: large-scale self-supervised pretraining for molecular property prediction. *arXiv preprint arXiv:2010.09885* **2020**,
- (21) Honda, S.; Shi, S.; Ueda, H. R. SMILES Transformer: Pre-trained Molecular Fingerprint for Low Data Drug Discovery. **2019**,
- (22) Fabian, B.; Edlich, T.; Gaspar, H.; Segler, M.; Meyers, J.; Fiscato, M.; Ahmed, M. Molecular representation learning with language models and domain-relevant auxiliary tasks. *arXiv preprint arXiv:2011.13230* **2020**,
- (23) Liu, P.; Ren, Y.; Tao, J.; Ren, Z. Git-mol: A multi-modal large language model for molecular science with graph, image, and text. *Computers in Biology and Medicine* **2024**, *171*, 108073.
- (24) Guo, T.; Guo, K.; Liang, Z.; Guo, Z.; Chawla, N. V.; Wiest, O.; Zhang, X., et al. What indeed can gpt models do in chemistry? a comprehensive benchmark on eight tasks. *arXiv preprint arXiv:2305.18365* **2023**, *16*.
- (25) Liu, S.; Du, W.; Ma, Z.-M.; Guo, H.; Tang, J. A group symmetric stochastic differential equation model for molecule multi-modal pretraining. International Conference on Machine Learning. 2023; pp 21497–21526.
- (26) Ai, Q.; Meng, F.; Shi, J.; Pelkie, B.; Coley, C. W. Extracting Structured Data from Organic Synthesis Procedures Using a Fine-Tuned Large Language Model. **2024**,
- (27) Yu, Q.; Zhang, Y.; Ni, Y.; Feng, S.; Lan, Y.; Zhou, H.; Liu, J. Multimodal Molecular Pretraining via Modality Blending. The Twelfth International Conference on Learning Representations. 2023.

- (28) Liu, S.; Nie, W.; Wang, C.; Lu, J.; Qiao, Z.; Liu, L.; Tang, J.; Xiao, C.; Anandkumar, A. Multi-modal molecule structure–text model for text-based retrieval and editing. *Nature Machine Intelligence* **2023**, *5*, 1447–1457.
- (29) Zeng, Z.; Yao, Y.; Liu, Z.; Sun, M. A deep-learning system bridging molecule structure and biomedical text with comprehension comparable to human professionals. *Nature communications* **2022**, *13*, 862.
- (30) Kim, S.; Thiessen, P. A.; Bolton, E. E.; Chen, J.; Fu, G.; Gindulyte, A.; Han, L.; He, J.; He, S.; Shoemaker, B. A., et al. PubChem substance and compound databases. *Nucleic acids research* **2016**, *44*, D1202–D1213.
- (31) Du, Z.; Qian, Y.; Liu, X.; Ding, M.; Qiu, J.; Yang, Z.; Tang, J. GLM: General Language Model Pretraining with Autoregressive Blank Infilling. Proceedings of the 60th Annual Meeting of the Association for Computational Linguistics (Volume 1: Long Papers). 2022; pp 320–335.
- (32) Ouyang, L.; Wu, J.; Jiang, X.; Almeida, D.; Wainwright, C.; Mishkin, P.; Zhang, C.; Agarwal, S.; Slama, K.; Ray, A., et al. Training language models to follow instructions with human feedback. *Advances in neural information processing systems* **2022**, *35*, 27730–27744.
- (33) Achiam, J.; Adler, S.; Agarwal, S.; Ahmad, L.; Akkaya, I.; Aleman, F. L.; Almeida, D.; Altenschmidt, J.; Altman, S.; Anadkat, S., et al. Gpt-4 technical report. *arXiv preprint arXiv:2303.08774* **2023**,
- (34) Wang, X.; Cheng, Y.; Yang, Y.; Yu, Y.; Li, F.; Peng, S. Multitask joint strategies of self-supervised representation learning on biomedical networks for drug discovery. *Nature Machine Intelligence* **2023**, *5*, 445–456.
- (35) David, L.; Thakkar, A.; Mercado, R.; Engkvist, O. Molecular representations in AI-

- driven drug discovery: a review and practical guide. *Journal of Cheminformatics* **2020**, *12*, 56.
- (36) Ertl, P. Molecular structure input on the web. *Journal of cheminformatics* **2010**, *2*, 1–9.
- (37) Landrum, G. Rdkit documentation. *Release* **2013**, *1*, 4.
- (38) O’Boyle, N. M.; Banck, M.; James, C. A.; Morley, C.; Vandermeersch, T.; Hutchison, G. R. Open Babel: An open chemical toolbox. *Journal of cheminformatics* **2011**, *3*, 1–14.
- (39) Li, Z.; Jiang, M.; Wang, S.; Zhang, S. Deep learning methods for molecular representation and property prediction. *Drug Discovery Today* **2022**, *27*, 103373.
- (40) Wang, Z.; Mi, J.; Lu, S.; He, J. MultiModal-Learning for Predicting Molecular Properties: A Framework Based on Image and Graph Structures. *arXiv preprint arXiv:2311.16666* **2023**,
- (41) Fink, T.; Reymond, J.-L. Virtual exploration of the chemical universe up to 11 atoms of C, N, O, F: assembly of 26.4 million structures (110.9 million stereoisomers) and analysis for new ring systems, stereochemistry, physicochemical properties, compound classes, and drug discovery. *Journal of chemical information and modeling* **2007**, *47*, 342–353.
- (42) Wang, M.; Wang, Z.; Sun, H.; Wang, J.; Shen, C.; Weng, G.; Chai, X.; Li, H.; Cao, D.; Hou, T. Deep learning approaches for de novo drug design: An overview. *Current opinion in structural biology* **2022**, *72*, 135–144.
- (43) Axelrod, S.; Gomez-Bombarelli, R. GEOM, energy-annotated molecular conformations for property prediction and molecular generation. *Scientific Data* **2022**, *9*, 185.
- (44) Yang, Z.; Huang, T.; Pan, L.; Wang, J.; Wang, L.; Ding, J.; Xiao, J. QuanDB: a

- quantum chemical property database towards enhancing 3D molecular representation learning. *Journal of Cheminformatics* **2024**, *16*, 48.
- (45) Polykovskiy, D.; Zhebrak, A.; Sanchez-Lengeling, B.; Golovanov, S.; Tatanov, O.; Belyaev, S.; Kurbanov, R.; Artamonov, A.; Aladinskiy, V.; Veselov, M., et al. Molecular sets (MOSES): a benchmarking platform for molecular generation models. *Frontiers in pharmacology* **2020**, *11*, 565644.
- (46) Irwin, J. J.; Shoichet, B. K. ZINC- a free database of commercially available compounds for virtual screening. *Journal of chemical information and modeling* **2005**, *45*, 177–182.
- (47) Gaulton, A.; Bellis, L. J.; Bento, A. P.; Chambers, J.; Davies, M.; Hersey, A.; Light, Y.; McGlinchey, S.; Michalovich, D.; Al-Lazikani, B., et al. ChEMBL: a large-scale bioactivity database for drug discovery. *Nucleic acids research* **2012**, *40*, D1100–D1107.
- (48) Ramakrishnan, R.; Dral, P. O.; Rupp, M.; Von Lilienfeld, O. A. Quantum chemistry structures and properties of 134 kilo molecules. *Scientific data* **2014**, *1*, 1–7.
- (49) Radford, A.; Kim, J. W.; Hallacy, C.; Ramesh, A.; Goh, G.; Agarwal, S.; Sastry, G.; Askell, A.; Mishkin, P.; Clark, J., et al. Learning transferable visual models from natural language supervision. International conference on machine learning. 2021; pp 8748–8763.
- (50) McCann, B.; Keskar, N. S.; Xiong, C.; Socher, R. The natural language decathlon: Multitask learning as question answering. *arXiv preprint arXiv:1806.08730* **2018**,
- (51) Kwiatkowski, T.; Palomaki, J.; Redfield, O.; Collins, M.; Parikh, A.; Alberti, C.; Epstein, D.; Polosukhin, I.; Devlin, J.; Lee, K., et al. Natural questions: a benchmark for question answering research. *Transactions of the Association for Computational Linguistics* **2019**, *7*, 453–466.
- (52) Wang, A.; Singh, A.; Michael, J.; Hill, F.; Levy, O.; Bowman, S. R. GLUE: A multi-task



benchmark and analysis platform for natural language understanding. *arXiv preprint arXiv:1804.07461* **2018**,

(53) Post, M. A call for clarity in reporting BLEU scores. *arXiv preprint arXiv:1804.08771* **2018**,

(54) Brown, T.; Mann, B.; Ryder, N.; Subbiah, M.; Kaplan, J. D.; Dhariwal, P.; Neelakantan, A.; Shyam, P.; Sastry, G.; Askell, A., et al. Language models are few-shot learners. *Advances in neural information processing systems* **2020**, *33*, 1877–1901.

# TOC Graphic

